Analysis of the Chemistry of Ni-Base Turbine Disk Superalloys Using An Alloys-By-Design Modeling Approach

DAVID J. CRUDDEN, BABAK RAEISINIA, NILS WARNKEN, and ROGER C. REED

The chemistry of the Ni-base superalloys used for turbine disks is critiqued by making use of the recently developed Alloys-By-Design computer-based tools. Compositions within the Ni-Cr-Co-Al-Ti-Mo-W-Ta(-Zr-C-B) design space are evaluated virtually. The assessment is made on the basis of sub-models for yield strength, creep behavior, oxidation resistance, and density; microstructural factors such as γ' volume fraction and γ' solvus temperature are considered where needed. The trade-offs between the different factors are studied in a quantitative sense. Diagrams are developed for the different alloy properties to highlight the limitations and challenges that one encounters when designing new grades of alloy or when optimizing existing grades. Composition-property maps are constructed that allow for an informed approach when defining an alloy composition. Specifically, the impact of chromium, molybdenum, and tungsten additions when mechanical behavior and lifing considerations are of concern is demonstrated.

DOI: 10.1007/s11661-012-1569-7

I. INTRODUCTION

Ni-BASE superalloys are remarkable for the range and number of alloying elements used in their constitution. Typical grades call for as many as ten alloying element additions. For example, (1) chromium and cobalt are added to promote resistance to oxidation and corrosion, (2) aluminum, titanium, and tantalum to impart precipitation hardening, (3) tungsten and rhenium to impart resistance to creep deformation, and (4) zirconium and boron for grain boundary strengthening. At least in part, this situation arises because nickel displays a capacity to dissolve significant quantities of its neighbors from the d-block of transition metals. In this way, one can argue that superalloys—as a class of structural alloys—possess a degree of chemical complexity which is rare and arguably unique. It has been pointed out recently[1] that this situation presents a challenge since the many possible alloying elements mean that the existing grades of Ni-base superalloys are unlikely to be optimized for their intended applications. Thus, alloy compositions superior to those currently available are likely to exist, waiting to be discovered or possibly be designed.

Traditionally, alloy design has invoked considerable use of trial and error-based approaches involving costly and exhaustive processing backed up by empirical property testing. Consider, for example, the development of alloy N18.[2] In this instance, alloys René 95, with its high strength, and Astroloy, with its superior resistance to crack propagation, were blended in various proportions with the aim of developing a more balanced alloy. In total, over 50 different alloy chemistries were evaluated to reach the chemistry of alloy N18, which was subsequently selected for more comprehensive, scaled-up evaluation.[3] The prevalent use of empirical methods in the design of Ni-base superalloys is also evident from Figure 1, in which the evolution of turbine disk alloy compositions patented over the past 50 years, binned into 5-year classes, is depicted. In this figure, each point represents the mean within each 5-year class and the whiskers point to the minimum and maximum in that class. It is clear that as time has progressed, no particular trend toward higher or lower levels of any of the alloying elements has occurred. This level of arbitrariness in the composition of the alloys, albeit in part, can be attributed to the reliance of alloy design methods on experience and empiricism.

Given the breadth of available alloy design space, one cannot hope to find new grades of superalloys by continuing the inefficient and costly past practices; it is crucial to take advantage of computer-based modeling and analysis tools that facilitate expedited identification of new grades of alloys and, ultimately, allow for a much closer integration of component design, manufacturing intent, and materials' aspects at greater cost-effectiveness. As materials' models and modeling strategies mature, in conjunction with development of reliable thermodynamic and kinetic databases, the utility of the noted tools in the design of superalloys is becoming all the more apparent; this is demonstrated by the works of Small and Saunders,[4] Tancret *et al.*,[5] Yokokawa *et al.*,[6] and Reed *et al.*[1]

In this paper, computer-based modeling and analysis tools are applied for the "virtual" characterization and evaluation of composition design spaces for Ni-base

DAVID J. CRUDDEN, Postgraduate Student, NILS WARNKEN, Lecturer, and ROGER C. REED, Director of Research, are with the School of Metallurgy and Materials, University of Birmingham, Edgbaston, Birmingham B15 2TT, U.K. Contact e-mail: djc000@bham.ac.uk BABAK RAEISINIA, Research Scientist, formerly with School of Metallurgy and Materials, University of Birmingham, and is now with Novelis Inc., Kennesaw, GA.

Manuscript submitted February 16, 2012.
Article published online December 14, 2012

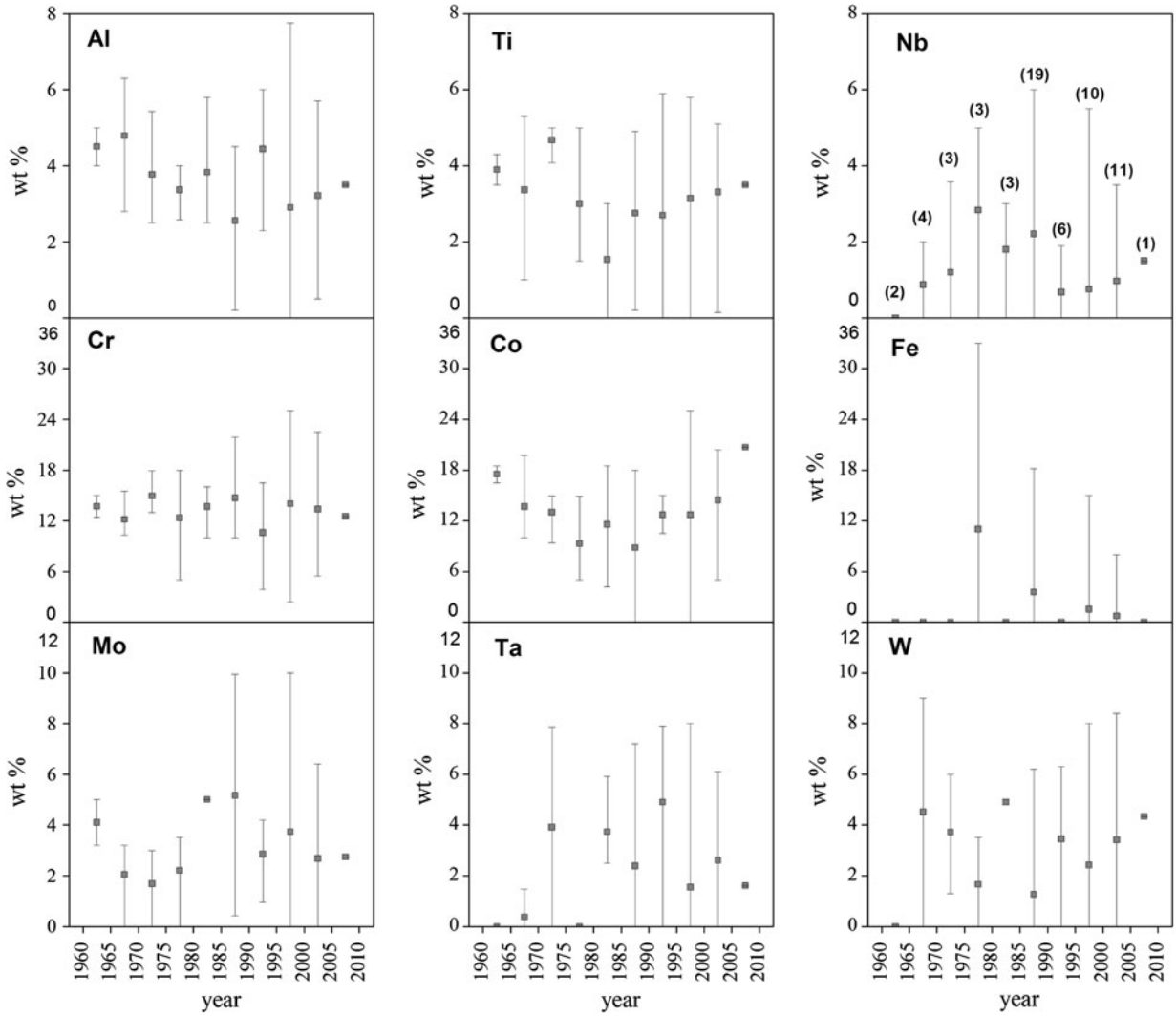

Fig. 1—Timeline of the chemistry of select patented Ni-base disk alloys binned into 5-year classes. The points represent the mean of the concentrations of the alloying elements in each class and the whiskers point to the maximum and minimum of the concentrations in the patents. The so-called "preferred" compositions are noted for each element. The numbers listed in parentheses on the Nb plot are the number of patents examined for each case. For example, 19 disk alloy patents were examined which were published between the years 1985 and 1990.

superalloys. An aim is to demonstrate the manner by which such methods allow quantitative relationships between alloy constitution and properties to be developed, so that future alloy development efforts might be guided. Attention is focused on the polycrystalline superalloys used for turbine disks, *e.g.*, those utilized in gas turbines for jet propulsion and power generation. Their primary role is to provide fixturing for the turbine blades, while maintaining their integrity under the demanding in-service conditions. We expand upon the Alloys-By-Design modeling framework,[1] which was recently applied to single-crystal superalloys; the present work complements this first effort. The paper is organized as follows: First, in Section II, a brief overview of the Alloys-By-Design framework is provided. The different models, merit indices, and modeling strategies used in this framework are described. In Section III, the results of the analysis are presented, demonstrating the various trade-offs that exist between different characteristics and properties of disk alloys. An assessment of the modeling approach, property trade-offs, and how the trade-offs may be managed are considered in Section IV. Finally, in Section V the concluding remarks are presented.

II. PROCEDURES AND MODELS

The basic premise of the Alloys-By-Design approach, see Reference 1, is the estimation of design-relevant properties across a very broad compositional space, so that alloy composition/property relationships can be identified. In principle, this allows the so-called inverse problem to be solved—the identification of the optimum alloy composition which best satisfies the given design constraints. Needed for success are property sub-models which are sensitive to alloy chemistry. The basic algorithm involves[1] (1) defining the compositional

design space over which the optimization is to be attempted, (2) choosing suitable compositional intervals over which the calculations are made, (3) calculation of composition and microstructure-dependent merit indices for each trial alloy composition, (4) assessment of each trial composition against the design constraints and elimination of unsuitable compositions, and (5) the sorting/ranking of remaining compositions and identification of optimized compositions.

Superalloys used for turbine disks must display a combination of strength—both static and time-dependent—and resistance to environmental degradation. Microstructural stability is also important. The original formulation of the Alloys-By-Design approach[1] was aimed at single-crystal superalloys for turbine blades. Although the working conditions for a turbine blade involve higher temperatures and lower stresses as compared to turbine disks, comparatively similar property requirements are demanded from the two, *e.g.*, low density and high creep resistance. Therefore, many of the models presented in Reference 1 are likely to be applicable and will be utilized here. In particular, use will be made of the creep and density models introduced in that paper, following Reference 1.

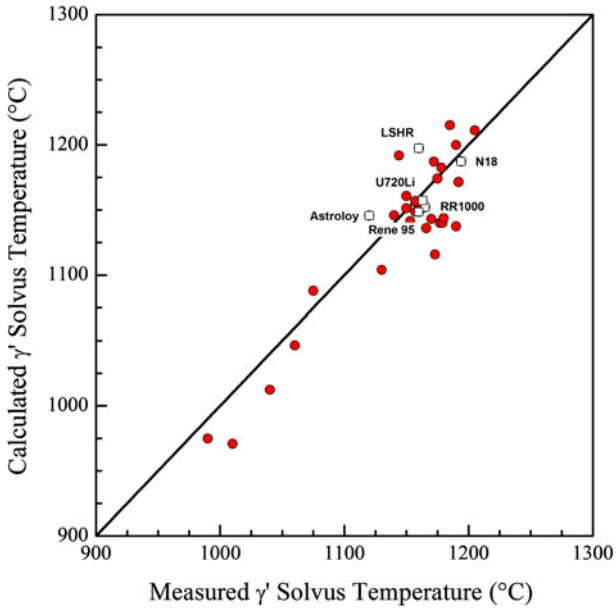

Fig. 2—Comparison of the calculated and measured γ' solvus temperatures for a number of different Ni-base superalloys. Measured values are those reported in the literature.[12–19] Select commercial alloys are indicated.

A. *Estimation of Phase Equilibria*

Both desirable and undesirable phases may form in nickel-based superalloys at various stages of their service life.[7] To determine the relative fraction of these phases for the different chemistries investigated, use here is made of Thermo-Calc coupled with the TTNI7 database.[8] The equilibrium calculations are performed at 923 K (650 °C), a temperature representative of typical operating conditions for a turbine disk. Two equilibrium calculations are performed per alloy composition: first, an equilibrium calculation to identify the phases present when the alloy enters into service and, second, an equilibrium calculation to identify the phases that form due to prolonged exposure to in-service temperature.

The state of the alloy when entering into service is simulated by assuming that only the γ (FCC-A1) and γ' phases are present. Thus, the mole fractions of these phases—taken to be approximately equal to their volume fraction—were calculated by imposing a two-phase equilibrium on the selected compositions. At this stage, no other phase was assumed to enter into the equilibrium. Note that the yield strength, creep resistance, and oxidation resistance calculations described later were all performed based on this equilibrium. The state of the alloy after a long period in service—where the stability of the alloy and its susceptibility to formation of topologically close-packed (TCP) phases is of concern—was simulated by assuming a three-phase γ, γ', and σ equilibrium. Once again, the presence of all other phases is suppressed by rejecting them at the onset of the equilibrium calculations. It is well documented that the σ phase formation significantly deteriorates the performance of Ni-base superalloys.[9] Recent work of Seiser *et al.*[10] has demonstrated that formation of the σ phase correlates strongly with the formation of other TCP phases; accordingly, only σ was considered in this work.

Thermo-Calc was also used to assess the γ' solvus temperature for each alloy composition. Consideration of the γ' solvus temperature serves as a measure of the processibility of the alloys; work by Gayda *et al.*[11] has demonstrated that there is a correlation between the quench crack susceptibility and the γ' solvus temperature. In this work, the solvus temperature is defined as the temperature at which the γ' volume fraction reaches zero. Figure 2 shows a comparison of γ' solvus temperatures taken from the literature[12–19] and those calculated in this work.

B. *Estimation of Yield Strength*

To the authors' knowledge, a theory-based composition-dependent yield strength model is not yet available for the nickel-based superalloys. Therefore, a Bayesian artificial neural network (ANN) following Reference 20 is used in the present work. The reader is referred to Reference 20 for a detailed description of the formulism of this ANN model. In brief, the model architecture utilized in this study consists of one hidden layer comprised of 32 hidden neurons. The hidden layer connects the inputs of the model (*i.e.*, alloy chemistry in wt pct, volume fraction of γ', and temperature) to the model output (*i.e.*, yield strength). A hyperbolic tangent function is used for the hidden neurons, due to its flexibility when fitting to data.[21]

To train and test the ANN model, the model made use of a database constructed from data contained within (1) the literature,[3,7,12,15,17,22–31] (2) commercial Ni-base superalloy datasheets (from The Special Metals Corporation and Haynes International Inc.), and (3) industrial patents.[14] The database contained information on 56 commercial and 69 experimental/development alloy compositions. Considering the different

temperatures taken into account for each of the 125 (= 56 + 69) compositions, a total of 428 unique cases were included in the database. Table I identifies each individual input for the neural network along with the corresponding maximum and minimum values within the training database. The model used a supervised training process, *i.e.*, the database was divided in half at random, allowing for a training and a test dataset. The final neural network considered 14 different alloying elements, the volume fraction of γ' in the alloy, and the test temperature as inputs. The γ' volume fraction is calculated using Thermo-Calc as described in Section II–A. Inclusion of the γ' volume fraction as an input into the model follows[32] where it was suggested that inclusion of this microstructural feature may improve the accuracy of the neural network's predictions.

Figure 3 shows the correlation between experimental and neural network predictions for the training and test data in the trained network.

Table I. Range of Input and Output Values Included in the Neural Network Database (Compositional Ranges are in Wt Pct)

Input	Range
Cr	31.50
Co	26.20
Mo	28.00
W	14.00
Ta	7.00
Nb	6.50
Al	5.00
Ti	6.20
Fe	45.00
Hf	2.00
C	0.95
B	0.20
Zr	0.50
γ'_{vf}	0.68
Temperature (°C)	21–800
Output	**Range**
Yield Strength (MPa)	165–1310

The minima are zero unless otherwise stated.

C. *Estimation of Oxidation Resistance*

Typical turbine disk alloys may contain between 10–20 wt pct of chromium. The chromium additions are made to improve oxidation resistance *via* the promotion of a protective chromia scale.[33–36] Accordingly, the relevant oxidation reaction for these alloys may be written:

$$\frac{4}{3}\mathrm{Cr} + \mathrm{O_2} \rightarrow \frac{2}{3}\mathrm{Cr_2O_3} \qquad [1]$$

The kinetics of chromia-scale growth may be described by Wagner's theory.[37] Based on this theory, the parabolic oxidation constant, k_t, is taken to be proportional to the Gibbs free energy of chromia formation, ΔG_f. Thus,

$$k_t \propto \Delta G_f \qquad [2]$$

Considering the chromia reaction presented in Eq. [1], Eq. [2] may be rewritten as

$$k_t \propto \left\{ \Delta G_o + RT \ln \left(\frac{a_{\mathrm{Cr_2O_3}}^{2/3}}{a_{\mathrm{Cr}}^{4/3} P_{\mathrm{O_2}}} \right) \right\} \qquad [3]$$

where ΔG_0 is the standard free energy of formation, R is the universal gas constant, T is the absolute temperature,

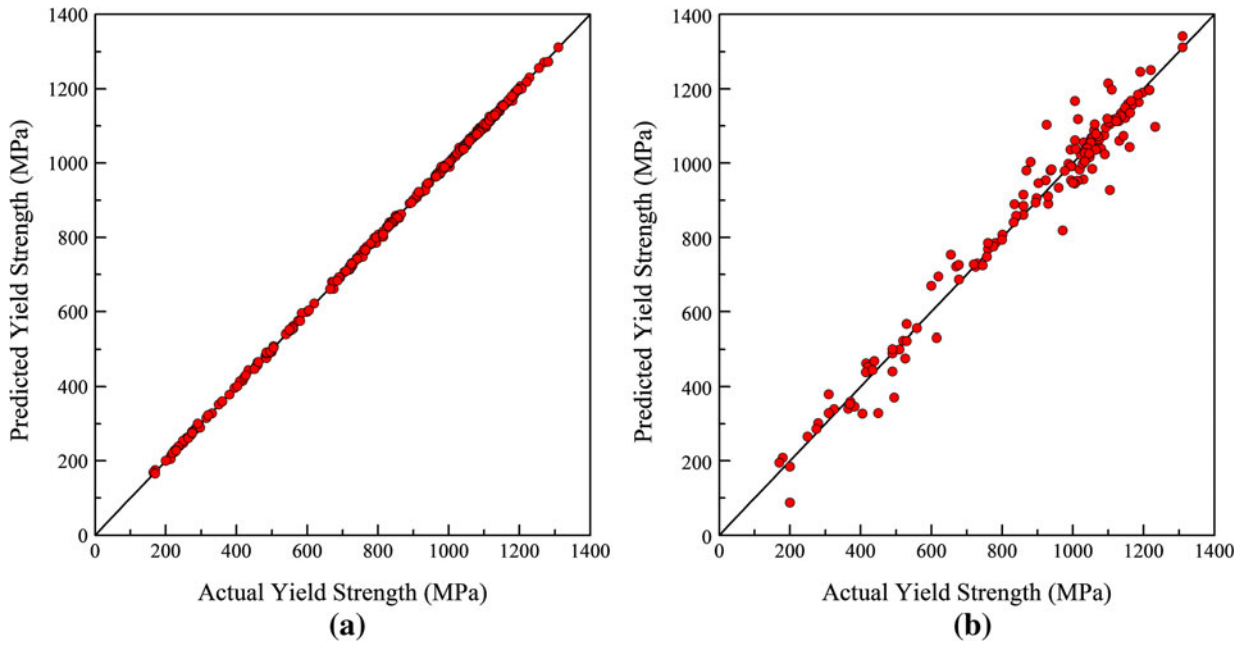

Fig. 3—Performance of the neural network compared with data contained in the (*a*) training set and (*b*) testing set.

Table II. List of Various Constants Used in This Work[38–40]

Element	D_0 (m^2/s)	Q (kJ/mol)	ρ (g/cm^3)
Cr	1.25×10^{-4}	267	7.220
Co	1.80×10^{-4}	282	8.900
Mo	8.53×10^{-4}	270	10.220
W	8.00×10^{-6}	264	19.300
Ta	2.19×10^{-5}	251	16.650
Al	1.87×10^{-4}	268	2.300
Ti	4.10×10^{-4}	275	4.508
Ni	—	—	8.902

$a_{Cr_2O_3}$ is the activity of chromia, a_{Cr} is the activity of chromium, and P_{O2} is the partial pressure of oxygen. Taking $a_{Cr_2O_3}$ to be unity and P_{O2} equal to 0.23 atm (in 1 atm of air), the parabolic oxidation constant is found to be inversely proportional to a_{Cr}. In this work, a_{Cr} is used as a measure for assessment and ranking of the oxidation response of different alloy chemistries. The higher the activity, the smaller the parabolic oxidation constant and, accordingly, the better the oxidation resistance. In this analysis, the activity of chromium is calculated for the alloy system of interest using Thermo-Calc with a two-phase equilibrium imposed.

D. *Estimation of Creep Resistance*

To rank the creep resistance of different alloy compositions, it is assumed that the unpinning of dislocations from pinned configurations is rate controlling. Following Reference 1 and assuming that the rate-controlling processes of diffusion represent a very first approximation, one writes

$$M_{creep} = \sum_i \frac{x_i}{D_i} \quad [4]$$

where x_i is the atomic fraction of solute i in the alloy and D_i is the interdiffusion coefficient for solute i with nickel. The interdiffusion coefficients are expressed by

$$D_i = D_{0i} \cdot \exp(-Q_i/RT) \quad [5]$$

where D_{0i} is a pre-exponential term, Q_i is the activation energy for diffusion, R is the universal gas constant (8.3145 J mol^{-1} K^{-1}), and T is the absolute temperature.

E. *Estimation of Density*

For the calculation of density, a simple rule-of-mixtures based on the densities of the pure elements and scaled by a factor of 1.05 is used, *i.e.*,

$$\rho = 1.05 \times \left[\sum_i x_i \rho_i\right] \quad [6]$$

following Reference 1. Here, x_i is the atomic faction of alloying element i and ρ_i is its density. The values for the different parameters introduced in the above equations are taken from the literature[38–40] and are provided in Table II.

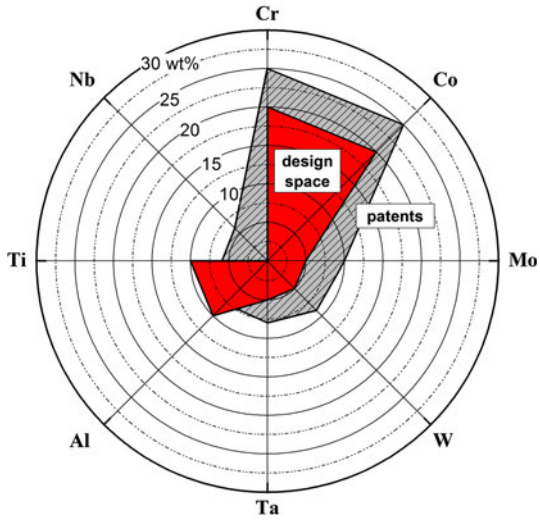

Fig. 4—Limits of the composition design space used in the present study (Table III). The extent of the patented compositional space for Ni-base disk alloys (Fig. 1) is also delineated.

Table III. Limits of the Composition Design Space Used in the Present Study

Element	Min Wt Pct	Max Wt Pct
Cr	15	20
Co	15	20
Mo	0	5
W	0	5
Ta	0	5
Al	1	8
Ti	1	10
Zr	0.06	0.06
C	0.027	0.027
B	0.015	0.015

III. RESULTS

The composition design space selected for the present analysis is the Ni-Cr-Co-Al-Ti-Mo-W-Ta system, illustrated in Figure 4. The alloying elements and their corresponding composition ranges are typical of industrial-grade turbine disk superalloys. Note that the present composition space lies within the patent space for disk alloys, Figure 4. In addition to the delineated elements, trace elements Zr, C, and B are also included in the analysis at fixed concentrations of 0.06, 0.027, and 0.015 wt pct, respectively. Noted in Table III are the composition limits considered in this work. To evaluate this space, the design space was randomly sampled while considering only whole-number (integer) wt pct variations for each of the elements. In total, in excess of 22,500 different compositions were analyzed within the bounds of the composition design space.

Figure 5 gives an overview of the trade-offs observed between the γ' volume fraction and the two predicted mechanical behavior characteristics studied here: yield strength and creep resistance. It can be seen from Figure 5(a) that there is a general trend toward higher

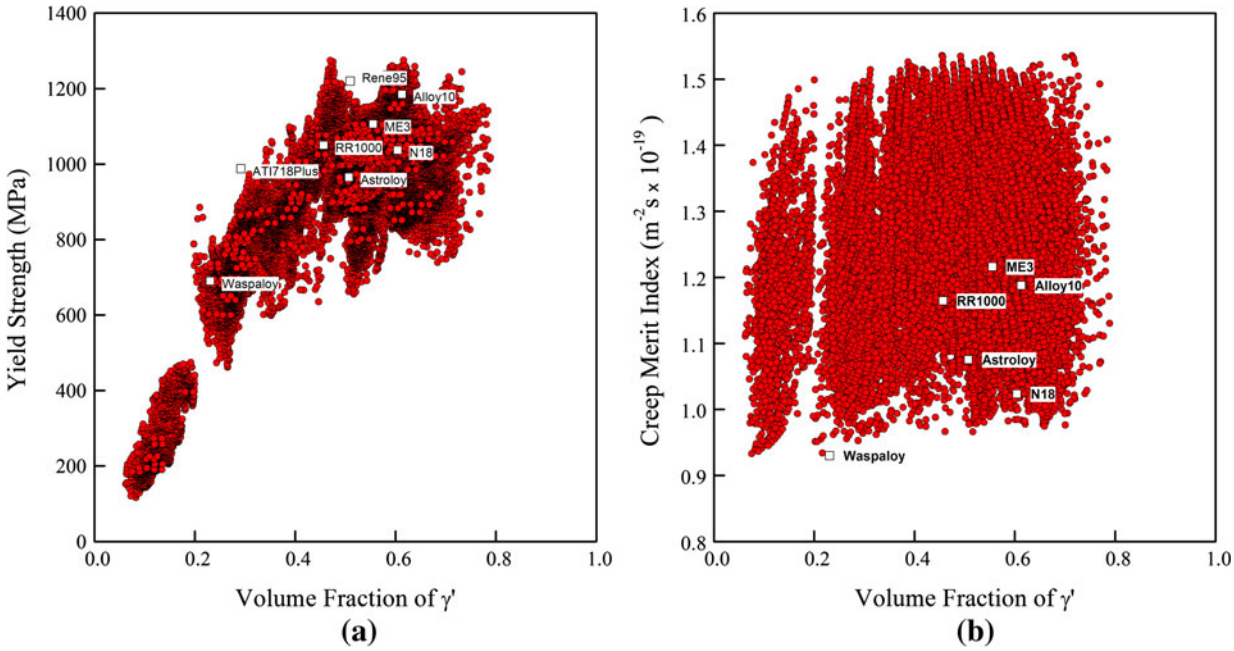

Fig. 5—Predicted (*a*) yield strength and (*b*) creep merit index as a function of γ' volume fraction at 923 K (650 °C).

yield strengths as the volume fraction of γ' in the alloys is raised. However, there is a spread in the yield strength values for a fixed volume fraction of γ'. This spread is especially notable for volume fractions greater than approximately 40 pct. At such high volume fractions, the overall correlation between the γ' volume fraction and yield strength becomes weaker. In contrast to the yield strength values, the calculated creep merit indices do not have any correlation with the volume fraction of γ', as shown in Figure 5(b).

Figure 6(a) shows that, in general, an increase in the γ' volume fraction results in a reduction of the density of the alloys. The data are, however, clustered into a number of distinct groups. A strong correlation between γ' content of the alloys and the γ' solvus temperature is also evident, as shown in Figure 6(b). Similar to yield strength, the dependence of γ' solvus temperature on γ' volume fraction becomes less pronounced beyond γ' volume fractions of 40 pct. Once again, at these volume fractions, there is an increase in the spread of γ' solvus temperature.

The trade-off between γ' volume fraction and volume fraction of σ phase (*i.e.*, alloy stability) is depicted in Figure 7(a). It is evident here that by increasing the γ' content of the alloy, the propensity of the alloy to detrimental σ phase formation also increases. A notable feature of this diagram is the significant spread in calculated properties. It is also important to note that at γ' contents greater than approximately 55 pct, formation of σ phase is unavoidable. Figure 7(b) shows that the stability of the alloy has a close correlation with the activity of chromium, a_{cr}, which as outlined in Section II–C is taken to be associated with an oxidation resistance. This figure shows that increasing the activity of chromium in the alloy makes the alloy more unstable. Care should, however, be taken in highlighting this general correlation given that, once again, there is a considerable spread in the data.

It is emphasized that the predicted values for a number of common industrial disk alloys are superimposed on all the aforementioned trade-off diagrams. These data points are included in the diagrams to highlight areas where improvements in present disk alloys may be attained.

IV. DISCUSSION

To deliver improved efficiency for future gas turbines, the thermal efficiency of the turbine's thermodynamic cycle must be increased. This is achieved using higher pressure ratios, higher turbine entry temperatures, and higher rotational speeds.[41] However, these goals cannot be met unless materials that can withstand such demanding conditions are identified. The alloys used for turbine disks are examples. The stress and temperature distribution across a turbine disk creates a demand for a mixture of high performance characteristics. High stresses at moderate temperatures in the hub of the disk demand high yield and tensile strengths combined with resistance to low cycle fatigue. The rim of the disk, operating at much higher temperatures, must have resistance to creep and stress rupture, as well as good tensile strength and dwell fatigue resistance.[42] These alloys must maintain their integrity in a demanding environment to deliver an acceptable component life. At these high temperatures, the alloy must remain stable and resist degradation due to corrosion and oxidation processes. Therefore, the overarching goal when designing new alloy chemistries is to achieve the highest temperature capability where reasonable component life is still achievable. In Section IV–A, the factors limiting the mechanical behavior of a turbine disk, particularly

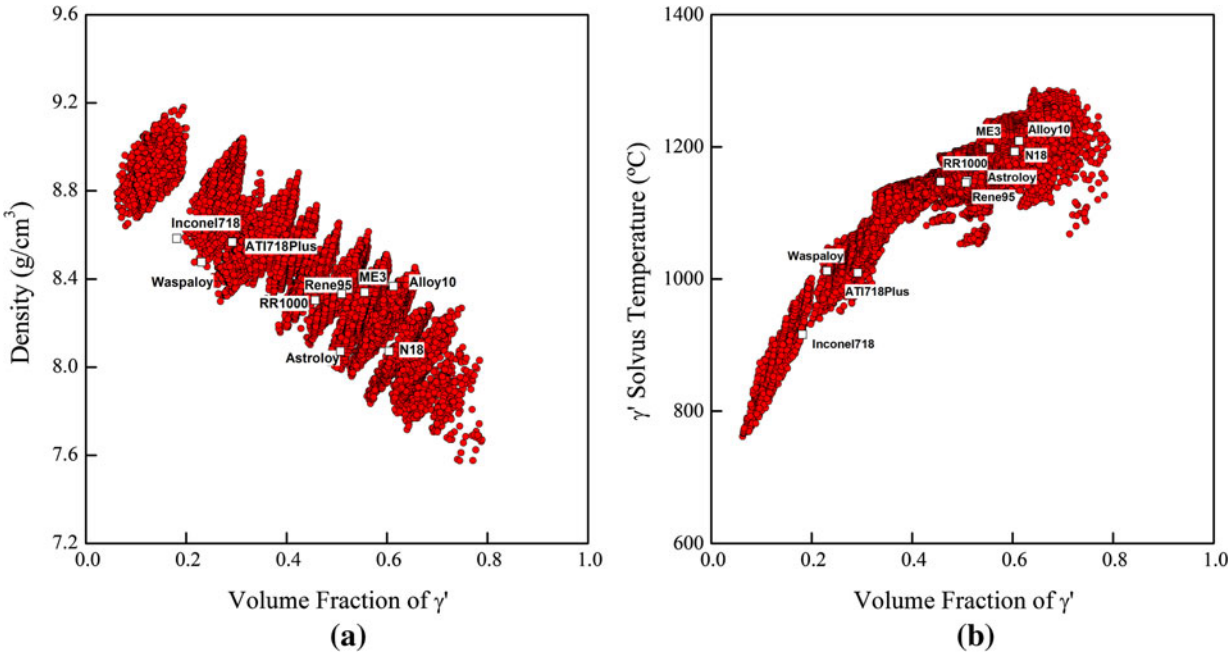

Fig. 6—Predicted (*a*) density and (*b*) γ' solvus temperature as a function of γ' volume fraction at 923 K (650 °C).

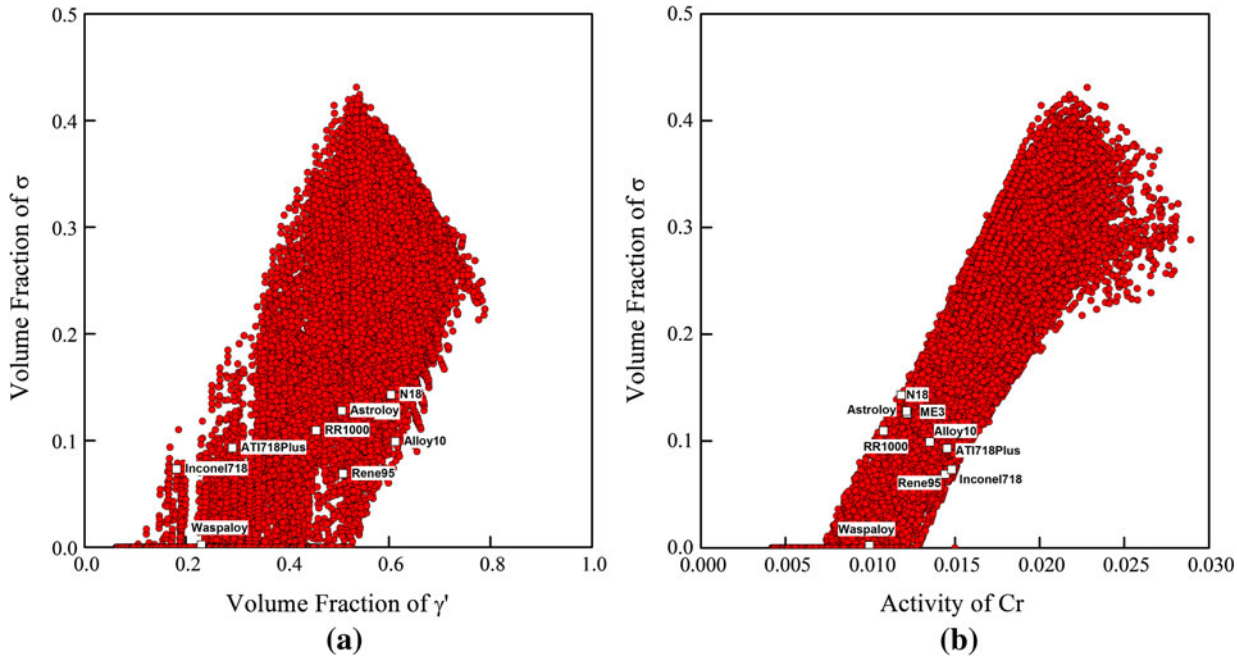

Fig. 7—Predicted σ volume fraction as a function of (*a*) γ' volume fraction and (*b*) chromium activity at 923 K (650 °C).

its yield strength, will be discussed and in Section IV–B, the factors which limit the life of a turbine disk alloy will be discussed.

A. *Mechanical Behavior Considerations in Design of Alloys*

Figure 5(a) demonstrates that at a given volume fraction of γ' , there can be a significant spread in alloy strength. For example, consider the locations of Astroloy and René 95 on this plot. These alloys have very similar γ' contents, but their yield strengths differ by approximately 160 MPa at 923 K (650 °C). Clearly, alloy chemistry is one of the main factors responsible for this variation in yield strength. In Figure 8(a), the impact of the molybdenum and tungsten content of the alloy on yield strength is depicted. It is evident here that at a fixed γ' volume fraction, molybdenum and tung-

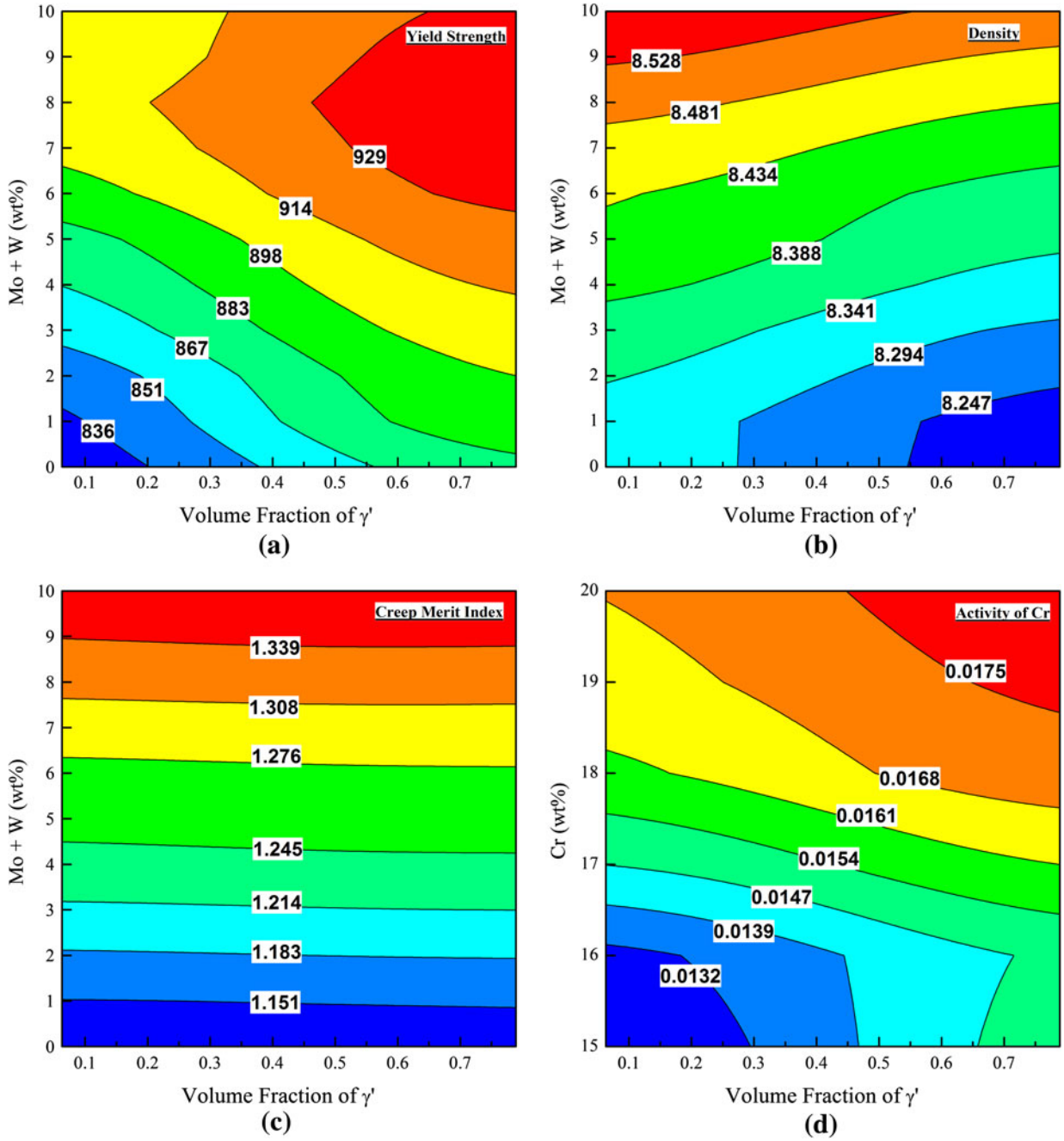

Fig. 8—Contour plots showing the effect of different alloying elements and γ' volume fraction on (*a*) the yield strength, (*b*) density in g/cm^3, (*c*) creep merit index in $m^{-2}s \times 10^{-19}$, and (*d*) activity of chromium.

sten—which predominantly partition to γ—increase the yield strength. This is in agreement with the experimental work by Mishima *et al.*[43] These authors found that among the elements which preferentially partition to the γ matrix, molybdenum and tungsten provided the most substantial solid solution strengthening effect. Similarly, Gayda and Gabb[44] observed that additions of up to 3 wt pct tungsten to disk alloy CH98 produced a 70 MPa increase in yield strength of the alloy at 977 K (704 °C). The beneficial effect of these elements in optimization of alloy strength is also reported in the development of alloy RR1000,[7] LSHR,[45] and Allvac 718.[46]

The spread in yield strength at a given volume fraction of γ', Figure 5(a), is too large to be explained solely by strengthening of the γ matrix. The overarching factor controlling this spread is most likely the chemistry of the γ' phase itself. Changes in the chemistry of γ' have an impact on the anti-phase boundary (APB) energy of this phase and, accordingly, on the precipitation strengthening effect of the alloy. Among the different

strengthening mechanisms in Ni-base superalloys, precipitation strengthening has been found to have a very pronounced effect, *cf.* Nembach[47] and Kozar *et al.*[48] Tantalum,[49] titanium,[50] and niobium[51] have been shown to increase the APB energy of the γ' phase. The APB energy strongly determines the magnitude of precipitate strengthening at a fixed volume fraction of γ'. This is evident from Eq. [7] which describes the maximum strengthening effect from the precipitates,[7]

$$\sigma_{y_{\text{peak}}} = \overline{M} \cdot \frac{1}{2} \gamma_{\text{APB}} f^{1/2} / b \qquad [7]$$

Here, $\sigma_{y\text{peak}}$ is the maximum yield strength contribution from precipitates, $\overline{M}$ is the average Taylor factor, γ_{APB} is the APB energy of γ', f is the volume fraction of γ', and b is the magnitude of the Burgers vector. It is hypothesized here that the variation in APB energy explains the increasing spread of yield strength at volume fractions of γ' greater than 40 pct as seen in Figure 5(a). As the γ' volume fraction increases, precipitation strengthening becomes the dominant strengthening mechanism, meaning the distribution in strength is then driven by variance in the APB energy. An example of how changing APB energy can be used in alloy design is highlighted in the development of NR3 alloy.[15] In this development, N18 was used as the base chemistry; the γ' content of the alloy was maintained, while its molybdenum was removed to improve stability. The aim was for NR3 to be as strong as N18; but, to counteract for the reduction in solution strengthening due to removal of molybdenum, an increase in the Ti/Al ratio (in at pct) from 0.6 to 0.9 was utilized.[15] The tensile properties of NR3 are equivalent to N18; this is possible because titanium additions raise the APB energy,[50] increasing the magnitude of strengthening from precipitates and, thus, balancing the loss in solid solution strengthening. It is to be noted here that the neural network used in this study does not explicitly account for APB energy or, for that matter, precipitation or solid solution strengthening effects. However, these effects are implicit in the database used for the training of the model.

Neural network models have found utility in predicting the yield and tensile strength of polycrystalline Ni-base superalloys, see *e.g.*, References 5, 32, and 52. Although a good approximation of alloy strength is achieved using this method, there is still a limit to the understanding which can be deduced from the model. To obtain a more comprehensive understanding of alloying effects on the yield strength of Ni-base superalloys, a phenomenological model can certainly provide a greater insight. In particular, such models would ideally allow the complicated correlation between chemistry, microstructure, and processing/service parameters to be evaluated. This is demonstrated in the recent work of Kozar *et al.*[48] These authors have successfully described the yield strength of IN100 by considering the various strengthening mechanisms that come into play in Ni-base superalloys and by explicitly taking into account the different microstructural features of superalloys that impact the yield strength (*e.g.*, size of precipitates). However, extending this work to other Ni-base superalloys does require further work as the chemistry dependence of the different variables of the model is yet to be established. In particular, the chemical dependance of APB energy. Although first-principles calculations[53] and thermodynamic modeling[54] have been applied to understand the chemical dependance of the APB, an increased understanding of this chemical dependance is certainly needed for future development of high strength Ni-base superalloys.

When developing an alloy for high strength, it is important to consider density as an input into specific strength. Figure 6(a) shows that an increase in γ' content reduces the density of the material. This decrease may be understood in terms of the increased additions of aluminum and titanium which are required to raise the γ' volume fraction of the alloy. This correlation between γ' content and density is highly advantageous as increasing γ' content will increase the yield strength, see Figure 5(a) and Eq. [7]. Another issue to be treated is that at a given volume fraction of γ', there is a spread in density. This spread in density is a consequence of the addition of heavy refractory elements molybdenum, tungsten, and tantalum. As shown in Figure 6(a), there is also a clustering of the data in this plot. These clusters represent the sum of Ti + Al; each cluster shows a small increase in γ' content with a corresponding increase in density. This correlation is explained by tantalum additions, which increase the volume fraction of γ' phase, but since it is heavier than nickel, it increases the density. Figure 8(b) shows that at a given volume fraction of γ', molybdenum and tungsten additions increase density. Cobalt and chromium additions have little effect on density as they have a density similar to that of nickel.

Having observed the above trade-offs and correlations, the obvious choice when designing a high strength, low density alloy would be to move toward higher γ' contents and to make little use of refractory elements. However, considering Figures 6(b) and 7(a), it can be seen that the γ' content must be selected with caution. A high γ' content is predicted to correspond to an increase in both the γ' solvus temperature and the susceptibility of the alloy to TCP phase, σ, formation. Considering that Figure 6(a) shows that the γ' content is related to the Ti + Al content, it is suggested that there is an upper limit to this value. As indicated earlier in Section II, work by Gayda *et al.*[11] showed that a high γ' solvus temperature makes an alloy more prone to quench cracking and, thus, makes its making processing more difficult. An alloy with a high propensity to σ formation will show a rapid deterioration in mechanical properties. Furthermore, the refractory elements are essential to improving creep resistance, Figure 8(c). It is, therefore, necessary to take all these considerations into account.

Figure 8(c) shows that for a given volume fraction of γ', the creep resistance increases with additions of tungsten and molybdenum. This agrees well with the experimental work conducted on CH98[44] where additions of 3 wt pct tungsten to CH98 gave a fivefold increase in 0.2 pct creep life at 977 K (704 °C). In the development of alloy ME3,[42] the importance of these

elements for creep resistance is also highlighted. It is noted there that a tungsten content between 2 and 4 wt pct and a molybdenum content of greater than 2 wt pct are required to maintain adequate creep resistance. The current creep model assumes that creep is a diffusion-controlled process. Therefore, as shown in Eq. [4], the elements which diffuse the slowest in nickel impart the greatest creep resistance. The results presented in Figure 5(b) suggest that the volume fraction of γ' has no influence on creep resistance. However, the size and distribution of γ' precipitates may lead to the operation of a variety of deformation mechanisms.[55] At the intermediate creep temperatures considered in this work, it is assumed that dislocation climb is the dominant deformation mechanism.[56] Inclusion of the effects of microstructure through a phenomenological model based upon sound theory does merit further investigation.

B. *Lifing Considerations in Design of Alloys*

Chromium is added in significant quantities to improve corrosion resistance, promoting the formation of a protective chromia scale.[33] Figure 8(d) shows the change in the activity of chromium at a given volume fraction of γ'. For a given volume fraction of γ', additions of chromium increase the activity of chromium in the system. Based on the merit index described earlier, it is predicted that an increase in the chromium activity will produce an improved oxidation resistance. This is consistent with observations of the Ni-Cr[57] and Ni-Cr-Al system[58] where increased levels of chromium improved the formation of a continuous chromia scale. In Figure 9, the a_{Cr} for the Ni-Cr compositions examined in Reference 57 is calculated; the increased chromium activity correlates with a reduction in the parabolic rate constant.

The assumption that oxidation resistance is purely controlled by chromium is rather crude. Although it does provide a basis for ranking oxidation performance, previous studies have shown that consideration must also be given to other active elements within the alloy system.[33–36] Upon oxidation, the structure and chemistry of the scale are much more complex than that assumed in the present study. In particular, it is understood that the aluminum and titanium contents of a superalloy also influence the oxidation response of the alloy. For example, Chen *et al.*[33] showed that a high titanium content can have a significant detrimental effect on the oxidation performance of an alloy. There is still more work required to characterize and model the oxidation resistance of different alloys based on their chemistry. We believe the work of Sato *et al.*[59] provides a good basis for such developments.

Figure 8 indicates that improvements to the mechanical properties and oxidation resistance can be met by high levels of alloying. This suggests that to develop alloys for the next generation of gas turbines, a higher degree of alloying is required. Figure 10(a) shows that the problem is perhaps more complex. Firstly, as shown in Figure 7(a), volume fractions of γ' beyond

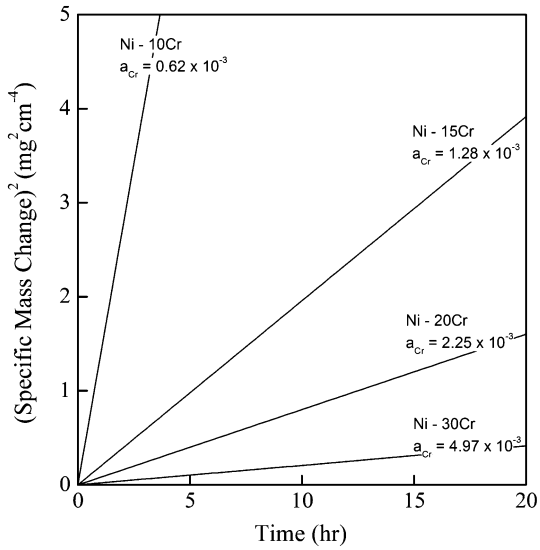

Fig. 9—Oxidation data for Ni-Cr binary alloys at 1173 K (900 °C) in 0.1 atm. of O_2, adapted from Ref. [57].

approximately 55 pct will lead to a high propensity to the precipitation of the σ phase. Also, depletion of nickel within the alloy raises the propensity to σ formation and this increase in instability due to excessive alloying might ultimately lead to an unacceptable component life. Figure 10(b) shows that, in particular, raising the molybdenum and tungsten content of the alloy for strength and creep resistance and chromium for improved oxidation will increase alloy instability. At a given volume faction of γ' , these elements must be used in balanced proportions as they contribute significantly to volume fractions of σ in the alloy. Past work has shown that reducing chromium levels can control stability; Udiment720Li was developed by reducing the chromium levels of Udimet720.[9] In the development of the RR1000 alloy, a balance had to be struck between the levels of chromium and molybdenum in the alloy;[41] chromium was maximized at the expense of molybdenum, meaning a reduction in high temperature strength and creep resistance.

C. *Example: Management and Optimization of Alloy Chemistries*

A close examination of Figures 8 and 10 shows that the minima and maxima delineated on these plots do not coincide with each other according to the design requirements. For example, the maximum yield strength region in Figure 8(a) is at the top right-hand corner, while the minimum density region in Figure 8(b) is at the bottom right-hand corner. This highlights the trade-off necessary between yield strength and density. The work presented in this paper is aimed at giving the reader guidance to make informed decisions when developing a new disk alloy. An example of how this approach can be implemented in the development of a new alloy, considering the outlined trade-offs, is presented below.

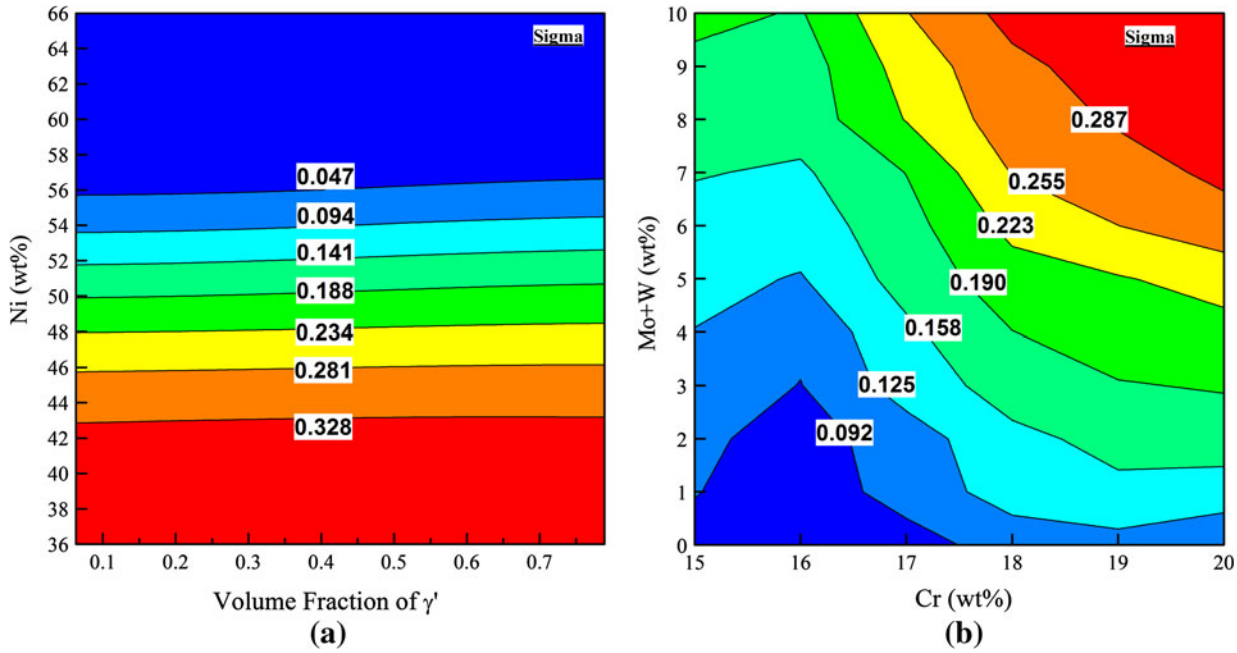

Fig. 10—Contour plots showing the variation of σ volume fraction with (*a*) nickel content and γ' volume fraction and (*b*) molybdenum, tungsten, and chromium content of the alloy.

Table IV. Range of Alloy Properties Predicted at Approximately 50 Pct Volume Fraction of γ'.

Property	Range
Yield Strength (MPa)	662–1186
Activity of Chromium	0.00949–0.02178
Creep Merit Index (m^{-2} s $\times$ 10^{-19})	0.977–1.51
Density (g/cm^2)	7.989–8.654
Volume Fraction of σ	0.0–0.4
γ' Solvus Temperature (°C)	1053–1198

In Section III, Figures 5, 6, and 7 demonstrate the importance of selecting an appropriate γ' content. Consider a γ' content of approximately 50 pct, which is typical of many recently developed disk alloys. This γ' content gives the designer a good range of values for material properties taken into account in this work, see Table IV. Once the γ' content has been selected, the trade-offs can be balanced considering Figures 8 and 10. Figure 11, which is a duplicate of Figure 10(b), highlights the key design options which can be made to optimize the alloy. The main limiting factor is the alloy stability. By reducing chromium content, the stability of the alloy can be improved, but oxidation resistance will be reduced as shown in Figure 8(d). Alternatively, by reducing the Mo + W content, stability will improve. However, strength and creep resistance will likely be lost, Figures 8(a) and (c). By changing both the Cr content and the Mo + W content, the designer can achieve a balanced trade-off, *i.e.*, a likely optimal alloy. It is to be noted here that the previous two sections demonstrate that the Alloys-By-Design predictions do align with empirical observations reported in the literature. It is, however, acknowledged that confirmation of predicted "optimal alloy" chemistries, as determined through the approach presented in this section, by experimental validation is necessary.

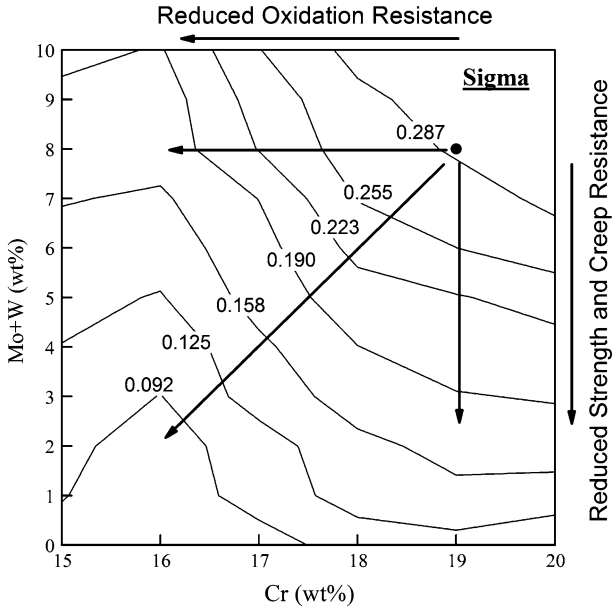

Fig. 11—A case study showing how the Alloys-by-Design method can be used to optimize alloy properties at a given volume fraction of γ'.

Finally, a note on the architecture of the Alloys-By-Design approach employed here. First, in this study, consideration is given only to the γ, γ', and σ phases. It is, however, acknowledged that a hierarchy of phases, desirable and undesirable, may form in these complex alloy systems. Many of these phases, even though not

present at high fractions, do have a pronounced effect on a number of properties. Consider, for example, the impact of carbides and borides on the mechanical response of Ni-base superalloys.[60–62] A comprehensive alloy design program does need to account for these phases; a necessity for such a goal to be realized is the availability of sound thermodynamic databases that can adequately model such phases. Second, there is still a large scope for integration of more models within the Alloys-By-Design approach to obtain a more comprehensive alloy design tool. Many properties which limit the success of a disk alloy still have to be understood, *e.g.*, fatigue crack propagation and resistance to sulfidation. Furthermore, models such as the yield strength model and the creep model presented in this work require further development to give greater insight into how chemistry controls these factors. True optimization of alloy chemistries will not be realized until our understanding of these properties is improved further.

V. SUMMARY AND CONCLUSIONS

The following conclusions can be drawn from this work:

1. The utility of an Alloys-by-Design modeling approach for the evaluation of compositional design spaces relevant to Ni-base superalloy turbine disks is demonstrated. The Ni-Cr-Co-Al-Ti-Ta-Mo-W (-Zr-C-B) system is considered, and alloys within this system are ranked based on their resistances to mechanical and environmental degradation and microstructural characteristics, *e.g.*, fraction of γ', γ' solvus temperature, propensity to σ precipitation.
2. The activity of chromium in an alloy is utilized as a measure of its resistance to oxidation. It is found that chromium additions correlate with improved oxidation resistance. However, a trade-off between improving oxidation resistance by this method and maintaining acceptable alloy stability exists.
3. A Bayesian ANN is used to predict the yield strength of the alloys as a function of their chemistry and temperature. The γ' volume fraction—estimated *via* Thermo-Calc calculations—is included as an additional input parameter into the neural network. The predicted yield strengths correlate with the concentration of molybdenum and tungsten in the alloys.
4. The propensity for σ phase formation (*i.e.*, a measure of alloy stability) is found to correlate closely with the level of alloying. A higher degree of alloying induces greater alloy instability. In particular, molybdenum, tungsten, and chromium are found to have a pronounced effect on instability.
5. The model predictions are used to construct chemistry-property maps. The maps demonstrate graphically the trade-offs that exist between different properties. These are useful for pedagogical pursues.
6. The application of the developed chemistry-dependent trade-off maps in optimization of Ni-base disk superalloy has been demonstrated *via* a number of examples.
7. The Alloys-by-Design methods are ultimately only as accurate as the underlying validity of the underlying sub-models and databases, *e.g.*, for thermodynamic properties. The methods are already valuable, but will become increasingly so as further improvements in the sub-models and the introductions of new ones are made to the system.

ACKNOWLEDGMENTS

The financial support of this work *via* the Engineering and Physical Sciences Research Council (EPSRC) of the United Kingdom and Rolls-Royce Strategic Partnership in Structural Metallic Systems for Advanced Gas Turbine Applications is greatly acknowledged. Fruitful and constructive discussions with Dr. Mark C. Hardy of Rolls-Royce plc are particularly appreciated. The authors would also like to thank Dr. Jean-Christophe Gebelin and Mr. Zailing Zhu at the University of Birmingham for their technical help.

REFERENCES

1. R.C. Reed, T. Tao, and N. Warnken: *Acta Mater.*, 2009, vol. 57, pp. 5898–5913.
2. C. Ducrocq, A. Lasalmonie, and Y. Honnorat: in *Superalloys 1988*, D.N. Duhl, G. Maurer, S. Antolovich, C. Lund, and S. Reichman, eds., TMS, Warrendale, PA, 1988, pp. 63–72.
3. J. Guedou, J. Lautridou, and Y. Honnorat: in *Superalloys 1992*, S.D. Antolovich, R.W. Stusrud, R.A. MacKay, D.L. Anton, T. Khan, R.D. Kissinger, and D.L. Klarstrom, eds., TMS, Warrendale, PA, 1992, pp. 267–76.
4. C.J. Small and N. Saunders: *MRS Bull.*, 1999, vol. 24, pp. 22–26.
5. F. Tancret, H.K.D.H. Bhadeshia, and D.J.C. MacKay: *Mater. Sci. Technol.*, 2003, vol. 19, pp. 283–90.
6. T. Yokokawa, H. Saeki, Y. Fukuyama, T. Yoshida, and H. Harada: *in Superalloys 2004*, K.A. Green, T.M. Pollock, H. Harada, T.E. Howson, R.C. Reed, J.J. Schirra, and S. Walston, eds., TMS, Warrendale, PA, 2004, pp. 859–66.
7. R.C. Reed: *The Superalloys: Fundamentals and Applications*, Cambridge University Press, Cambridge, 2006.
8. N. Saunders: in *Superalloys 1996*, R.D. Kissinger, D.J. Deye, D.L. Anton, A.D. Cetel, M.V. Nathal,T.M. Pollock, and D.A. Woodford., eds.,TMS, Warrendale, PA, 1996, pp. 101–10.
9. P.W. Keefe, S.O. Mancuso, and G.E. Maurer: in *Superalloys 1992*, S.D. Antolovich, R.W. Stusrud, R.A. MacKay, D.L. Anton, T. Khan, R.D. Kissinger, and D.L. Klarstrom, eds., TMS, Warrendale, PA, 1992, pp. 487–96.
10. B. Seiser, R. Drautz, and D.G. Pettifor: *Acta Mater.*, 2011, vol. 59, pp. 749–63.
11. J. Gayda, P. Kantzos, and J. Miller: *J. Fail. Anal. Prev.*, 2003, vol. 3, pp. 55–59.
12. J.Y. Guedou, I. Augustins-Lecallier, L. Naze, P. Caron, and D. Locq: in *Superalloys 2008*, R.C. Reed, K.A. Green, P. Caron, T.P. Gabb, M.G. Fahrmann, and E.S. Huron, eds.,TMS, Warrendale, PA, 2008, pp. 21–30.
13. J. Radavich, D. Furrer, T. Carneiro, and J. Lemsky: in *Superalloys 2008*, R.C. Reed, K.A. Green, P. Caron, T.P. Gabb, M.G. Fahrmann, and E.S. Huron, eds.,TMS, Warrendale, PA, 2008, pp. 63–72.
14. T.P. Gabb, J. Gayda I. Telesman, and P.T. Kantzos: US Patent 6974508, 2005.
15. D. Locq, M. Marty, and P. Caron: in *Superalloys 2000*, T.M. Pollock, R.D. Kissinger, R.R. Bowman, K.A Green, M. McLean,

S.L. Olson, and J.J Schirra, eds., TMS, Warrendale, PA, 2000, pp. 395–403.
16. S.J. Hessel, W. Voice, A.W. James, S.A. Blackham, C.J. Small, and M.R. Winstone: US Patent 6132527, 2000.
17. M. J. Donachie and S.J Donachie: *Superalloys: A Technical Guide*, ASM Internation, Materials Partk, OH, 2002.
18. R.N. Jarrett and J.K. Tien: *Metall. Trans A*, 1982, vol. 13A, pp. 1021–32.
19. C.Y. Cui, Y.F. Gu, D.H. Ping, and H. Harada: *Metall. Mater. Trans. A*, 2009, vol. 40A, pp. 282–91.
20. R.M. Neal: *Software for Flexible Bayesian Modelling and Markov Chain Sampling*, Ph.D. thesis, University of Toronto.
21. H.K.D.H. Bhadeshia: *ISIJ Int*., 1999, vol. 39, pp. 966–79.
22. E.S. Huron, K.R. Bain, D.P. Mourer, and T.P. Gabb: in *Superalloys 2008*, R.C. Reed, K.A. Green, P. Caron, T.P. Gabb, M.G. Fahrmann, and E.S. Huron, eds.,TMS, Warrendale, PA, 2008, pp. 181–89.
23. Y. Gu, H. Harada, C. Cui, D. Ping, A. Sato, and J. Fujioka: *Scripta Mater*., 2006, vol. 55, pp. 815–18.
24. R.J.D. Furrer: in *Superalloys 2004*, K.A. Green, T.M. Pollock, H. Harada, T.E. Howson, R.C. Reed, J.J. Schirra, and S. Walston, eds.,TMS, Warrendale, PA, 2004, pp. 381–90.
25. Nickel Development Institute, Birmingham England: *High Temperature High Strength Nickel Base Alloys*, Inco Alloys International Ltd., Huntington.
26. W.B. Kent: NASA/CR-135131 *NASA*, Lewis Research Centre, 1977.
27. J. Gayda: NASA/TM-2003-212471 *NASA*, Glenn Research Center, 2003.
28. J. Gayda: NASA/TM-2001-210814 *NASA*, Glenn Research Centre, 2001.
29. D. Ellis, T.P. Gabb, and A. Garg: NASA/TM-2004-213140 *NASA*, Glenn Research Centre, 2004.
30. T.P. Gabb, P.T. Kantzos, and K. O'Connor: NASA/TM-2002-211796 *NASA*, Glenn Research Centre, 2002.
31. J.R. Davis: *Nickel, Cobalt and Their Alloys*, ASM International, Materials Park, OH, 2000.
32. J. Jones and D.J.C. MacKay: in *Superalloys 1996*, R.D. Kissinger, D.J. Deye, D.L. Anton, A.D. Cetel, M.V. Nathal, T.M. Pollock, and D.A. Woodford., eds., TMS, Warrendale, PA, 1996, pp. 417–24.
33. H. Chen J, P.M. Rogers, and J.A. Little: *Oxid. Met*., 1997, vol. 47, pp. 381–410.
34. A. Encinas-Oropes, G.L. Drew, M.C. Hardy, A.J. Leggett, J.R. Nicholls, and N.J. Simms: in *Superalloys 2008*, R.C. Reed, K.A. Green, P. Caron, T.P. Gabb, M.G. Fahrmann, and E.S. Huron, eds., TMS, Warrendale, PA, 2008, pp. 609–18.
35. L. Zheng, M.C. Zhang, and J.X. Dong: *Appl. Surf. Sci.*, 2010, vol. 256, pp. 7510–15.
36. K.A. Al-hatab, M.A. Al-bukhaiti, U. Krupp, and M. Kantehm: *Oxid. Met*., 2011, vol. 75, pp. 209–28.
37. C. Wagner: *Z. Phys. Chem. B.Chem. E*, 1933, vol. 21, pp. 25–41.
38. M.S.A. Karunaratne, P. Carter, and R.C. Reed: *Mater. Sci. Eng. A Struct*., 2000, vol. 281, pp. 229–33.
39. M.S.A Karunaratne and R.C. Reed: *Acta Mater*., 2003, vol. 51, pp. 2905–19.
40. M. Krčmar, C.L. Fu, A. Janotti, and R.C. Reed: *Acta Mater*., 2005, vol. 53, pp. 2369–76.
41. M. Hardy, B. Zirbel, G. Shen, and R. Shankar: in *Superalloys 2004*, K.A Green, T.M Pollock, H. Harada, T.E. Howson, R.C. Reed, J.J. Schirra, and S. Walston, eds.,TMS, Warrendale, PA, 2004, pp. 83–90.
42. D.P. Mourer, E.S. Huron, K.R. Bain, E.E. Montero, P.L. Reynolds, and J.J. Schirra: US Patent 6521175B1, 2003.
43. Y. Mishima, S. Ochial, N. Hamou, M. Yodogawa, and T. Suzuki: *Trans. JIM*, 1986, vol. 27, pp. 656–64.
44. J. Gayda and T.P. Gabb: NASA/TM-2003-212474 *NASA*, Glenn Research Center, 2003.
45. T.P. Gabb, J. Gayda, I. Telesman, and P.T. Kantzos: US Patent 6974508B1, 2005.
46. W. Cao: US Patent 6730264B2, 2004.
47. E. Nembach: *Mater. Sci. Eng. A Struct*., 2006, vol. 429, pp. 277–86.
48. R.W. Kozar, A. Suzuki, W.W. Milligan, J.J. Schirra, M.F. Savage, and T.M. Pollock: *Metall. Mater. Trans. A*, 2009, vol. 40A, pp. 1588–603.
49. N. Baluc, H.P. Karnthaler, and M.J. Mills: *Philos. Mag. A*, 1991, vol. 64, pp. 137–50.
50. D. Raynor and J. M. Silcock: *Met. Sci*, 1970, vol. 4, pp. 121–30.
51. E.C. Guo and F.J. Ma: in *Superalloys 1980*, J.K. Tien, S.T. Wlodek, H. Morrow III, M. Gell, and G.E. Maurereds, eds, TMS, Warrendale, PA, 1980, pp.431–38.
52. I. Di Martino, J.W. Brooks, P.A.S. Reed, P. Holdway, and A. Wisbey: *Mater. Sci. Technol*., 2007, vol. 23, pp. 1402–07.
53. M. Chandran and S.K. Sondhi: *Model. Simul. Mater. Sci*., 2011, vol. 19, pp. 1–7.
54. A.P. Miodownik and N.J. Saunders: in *Applications of Thermodynamics in the Synthesis and Processing of Materials*, P. Nash and B. Sundman, eds., TMS, Warrendale, PA, 1995 pp. 91–104.
55. R.R. Unocic, G.B. Viswanathan, P.M. Sarosi, S. Karthikeyan J. Li, and M.J. Mills: *Mater. Sci. Eng. A Struct*., 2008, vol. 483, pp. 25–32.
56. T.M. Pollock and S. Tin: *J. Propul. Power*., 2006, vol. 22, pp. 361–74.
57. C.S. Giggins and F.S. Pettit: *Trans. AIME*, 1969, vol. 245, pp. 2495–507.
58. C.S. Giggins and F. S. Pettit: *J. Electrochem. Soc*., 1971, vol. 118, pp. 1782–90.
59. A. Sato, Y.L. Chiu, and R.C. Reed: *Acta Mater*., 2011, vol. 59, pp. 225–40.
60. Q.Z. Chen, N. Jones, and D.M. Knowles: *Acta Mater*., 2002, vol. 50, pp. 1095–112.
61. E.S. Huron, K.R. Bain, D.P. Mourer, J.J. Schirra, P.L. Reynolds, and E.E. Montero: in *Superalloys 2004*, K.A Green, T.M Pollock, H. Harada, T.E. Howson, R.C. Reed, J.J. Schirra, and S. Walston, eds.,TMS, Warrendale, PA, 2004, pp. 73–81.
62. T.J. Garosshen, T.D. Tillman, and G.P. McCarthy: *Metall. Trans. A*, 1987, vol. 18A, pp. 69–77.